Optimal Design of Two-Channel Recursive Parallelogram Quadrature Mirror Filter Banks

Ju-Hong Lee, Yi-Lin Shieh

Abstract—This paper deals with the optimal design of two-channel recursive parallelogram quadrature mirror filter (PQMF) banks. The analysis and synthesis filters of the PQMF bank are composed of two-dimensional (2-D) recursive digital all-pass filters (DAFs) with nonsymmetric half-plane (NSHP) support region. The design problem can be facilitated by using the 2-D doubly complementary half-band (DC-HB) property possessed by the analysis and synthesis filters. For finding the coefficients of the 2-D recursive NSHP DAFs, we appropriately formulate the design problem to result in an optimization problem that can be solved by using a weighted least-squares (WLS) algorithm in the minimax (L_∞) optimal sense. The designed 2-D recursive PQMF bank achieves perfect magnitude response and possesses satisfactory phase response without requiring extra phase equalizer. Simulation results are also provided for illustration and comparison.

Keywords—Parallelogram Quadrature Mirror Filter Bank, Doubly Complementary Filter, Nonsymmetric Half-Plane Filter, Weighted Least Squares Algorithm, Digital All-Pass Filter.

I. INTRODUCTION

TWO-DIMENSIONAL (2-D) quadrature mirror filter (QMF) banks have been widely considered for high quality coding of image and video data at low bit rates and spatial image analysis like feature extraction and matching [1], [2]. The design problem of 2-D QMF banks with the perfect reconstruction (PR) characteristics has been considered in the literature [3], [4].

A parallel structure using the 2-D recursive NSHP DAF to construct the analysis and synthesis filters of a recursive two-channel parallelogram QMF (PQMF) bank has been presented in [5]. For image processing, the 2-D DC-based PQMF bank can avoid transmission nulls [6] without using additional delays and satisfy the frequency constraints [7], [8] that avoid the aliasing artifacts. However, an extra NSHP DAF used as a phase equalizer must be added in the synthesis system to eliminate the phase distortion induced by the 2-D recursive NSHP DAFs in the analysis and synthesis systems [5].

In this paper, we present a novel method for the minimax design of two-channel recursive PQMF banks using 2-D

recursive NSHP DAFs. The proposed 2-D recursive PQMF bank possesses the advantages as those presented by [5], namely, (i) the resulting analysis/synthesis filters possess the 2-D DC properties, i.e., 2-D all-pass complementary and power complementary properties, (ii) the proposed 2-D DC-based analysis/synthesis filters possess an attractive DC symmetry with respect to the half-band frequency $(\omega_1,\omega_2) = (0,\pi/2)$ in the upper half plane of the frequency plane, (iii) the proposed 2-D DC-based recursive PQMF bank have no magnitude distortion. The frequency characteristics totally depend on the phase responses of the 2-D recursive NSHP DAFs. However, the proposed 2-D recursive PQMF bank avoids the need of extra NSHP DAF used as a phase equalizer like [5] to achieve satisfactory linear-phase response. Using the stability constraints presented by [9] to guarantee the stability of the 2-D recursive NSHP DAFs, we then derive a novel objective function for minimax phase approximation. The problem of minimizing the objective function can be solved by using the weighted least-squares algorithm developed in [10] (termed as the LLCY algorithm). Simulation results show that the proposed design method provides more satisfactory results than the method of [5].

II. PROBLEM FORMULATION

A. PQMF Bank with Linear-Phase Response

The conventional 2-D two-channel PQMF system is shown in Fig. 1, where $H_0(z_1,z_2)$ and $H_1(z_1,z_2)$ are the low-pass and high-pass analysis filters, respectively, $F_0(z_1,z_2)$ and $F_1(z_1,z_2)$ are the low-pass and high-pass synthesis filters, respectively. **M** denotes the decimation/interpolation matrix. The ideal frequency specifications for the 2-D two-channel analysis and synthesis systems are given in Fig. 2. Setting the synthesis filters $F_0(z_1,z_2) = H_1(z_1, - z_2)$, $F_1(z_1,z_2) = - H_0(z_1, - z_2)$, and using the mirror-image symmetry about the frequency $(\omega_1,\omega_2) = (0,\pi/2)$, we have $H_1(z_1,z_2) = H_0(z_1, - z_2)$ and the input/output relationship of the 2-D PQMF bank in the z-transform as follows:

$$\hat{X}(z_1,z_2) = \frac{1}{2}\left[H_0^2(z_1,z_2) - H_0^2(z_1,-z_2)\right]X(z_1,z_2) \tag{1}$$

Let $T(e^{j\omega_1},e^{j\omega_2}) = H_0^2(e^{j\omega_1},e^{j\omega_2}) - H_0^2(e^{j\omega_1},e^{j(\omega_2+\pi)})$ be the frequency response of the PQMF bank. Equation (1) reveals that producing an output $\hat{x}(m,n)$ that is a delayed replica of $x(m,n)$ requires

This work was supported by the National Science Council under Grant NSC100-2221-E002-200-MY3.

J.-H. Lee is with the Department of Electrical Engineering, Graduate Institute of Communication Engineering, National Taiwan University, No.1, Sec.4, Roosevelt Rd., Taipei 10617 Taiwan (phone: 886-2-23635251; fax: 886-2-23671909; e-mail: jhlee@ntu.edu.tw).

Y.-L. Shieh is with the Graduate Institute of Communication Engineering, National Taiwan University, No.1, Sec.4, Roosevelt Rd., Taipei 10617 Taiwan (e-mail: r97942105@ntu.edu.tw).

World Academy of Science, Engineering and Technology
International Journal of Computer and Information Engineering
Vol:8, No:7, 2014

$$T(e^{j\omega_1}, e^{j\omega_2}) = \frac{H_0^2(e^{j\omega_1}, e^{j\omega_2}) - H_0^2(e^{j\omega_1}, e^{j(\omega_2+\pi)})}{2} = e^{-j(g_1\omega_1 + g_2\omega_2)}, \quad (2)$$

for $\forall (\omega_1, \omega_2)$, where g_1 and g_2 are the system delays of the PQMF bank. Designing of PQMF banks with conventional FIR or IIR structures for $H_0(z_1, z_2)$ usually induces both magnitude and phase distortions.

B. Digital All-Pass Based PQMF Bank

First, we use the widely considered decimation/interpolation matrix $\mathbf{M} = \begin{bmatrix} 1 & -1 \\ 0 & 2 \end{bmatrix}$. Then, a new two-channel recursive PQMF bank is constructed by setting the analysis filters $H_0(z_1, z_2)$ and $H_1(z_1, z_2)$ of Fig. 1 as follows:

$$H_0(z_1, z_2) = \frac{A_1(z_1, z_2) + z_2^{-1} A_2(z_1, z_2)}{2}$$

$$H_1(z_1, z_2) = \frac{A_1(z_1, z_2) - z_2^{-1} A_2(z_1, z_2)}{2} \quad (3)$$

where $A_i(z_1, z_2)$, for $i = 1, 2$, are two 2-D DAFs with transform function given by

$$A_i(z_1, z_2) = z_1^{-M_i} z_2^{-N_i} \frac{D_i(z_1^{-1}, z_2^{-1})}{D_i(z_1, z_2)}, \quad (4)$$

where the denominator polynomial $D_i(z_1, z_2)$ of the $(M_i \times N_i)$th-order DAF $A_i(z_1, z_2)$ with nonsymmetric half-plane (NSHP) support regions for its coefficients is given by

$$D_i(z_1, z_2) = \sum_{m=0}^{M_i} d_i(m,0) z_1^{-m} + \sum_{m=-M_i}^{M_i} \sum_{n=1}^{N_i} d_i(m,n) z_1^{-m} z_2^{-n}$$

$$= \sum_{(m,n) \in \Re_i} d_i(m,n) z_1^{-m} z_2^{-n} \quad (5)$$

where $\Re_i$ represents the 2-D NSHP region on the 2-D (m,n) plane. We note from (3) and (4) that

$$\left| H_0(e^{j\omega_1}, e^{j\omega_2}) + H_1(e^{j\omega_1}, e^{j\omega_2}) \right| = 1, \quad \text{for } \forall (\omega_1, \omega_2),$$

$$\left| H_0(e^{j\omega_1}, e^{j\omega_2}) \right|^2 + \left| H_1(e^{j\omega_1}, e^{j\omega_2}) \right|^2 = 1, \text{ for } \forall (\omega_1, \omega_2), \quad (6)$$

Hence, $H_0(z_1, z_2)$ and $H_1(z_1, z_2)$ simultaneously satisfy the all-pass complementary and power complementary properties, i.e., $H_0(z_1, z_2)$ and $H_1(z_1, z_2)$ form a 2-D doubly-complementary (DC) filter pair. The $H_0(z_1, z_2)$ and $H_1(z_1, z_2)$ of Fig. 1 are replaced by (3) to form a new 2-D DC-based recursive PQMF bank of Fig. 3. From (1) and (3), we can show that the proposed 2-D two-channel PQMF bank has the transfer function given by

$$T(z_1, z_2) = \frac{1}{2} \left[H_0^2(z_1, z_2) - H_1^2(z_1, z_2) \right] = \frac{1}{2} z_2^{-1} A_1(z_1, z_2) A_2(z_1, z_2). \quad (7)$$

Equation (7) reveals that the 2-D two-channel recursive PQMF bank possesses a magnitude response without distortion.

C. Frequency Characteristics of 2-D DC Analysis Filters

The frequency response of (4) with phase response $\theta_i(\omega_1, \omega_2)$ can be expressed by

$$A_i(e^{j\omega_1}, e^{j\omega_2}) = e^{j\theta_i(\omega_1, \omega_2)} = e^{j[-M_i\omega_1 - N_i\omega_2 - 2\phi_i(\omega_1, \omega_2)]}, \quad (8)$$

where

$$\phi_i(\omega_1, \omega_2) = \arg\left\{ D_i(e^{j\omega_1}, e^{j\omega_2}) \right\} = -\left[M_i\omega_1 + N_i\omega_2 + \theta_i(\omega_1, \omega_2) \right]/2$$

$$= -\tan^{-1}\left\{ \frac{\sum\limits_{(m,n) \in \Re_i} d_i(m,n) \sin(m\omega_1 + n\omega_2)}{\sum\limits_{(m,n) \in \Re_i} d_i(m,n) \cos(m\omega_1 + n\omega_2)} \right\} \quad (9)$$

is the phase of $D_i(z_1, z_2)$. Substituting (8) into (3), we have

$$H_0(e^{j\omega_1}, e^{j\omega_2}) = \frac{1}{2}\left[A_1(e^{j\omega_1}, e^{j\omega_2}) + e^{-j\omega_2} A_2(e^{j\omega_1}, e^{j\omega_2}) \right] = \frac{1}{2}\left[e^{j\theta_1(\omega_1,\omega_2)} + e^{-j\omega_2} e^{j\theta_2(\omega_1,\omega_2)} \right]$$

$$= \cos\left[-\frac{M_1 - M_2}{2}\omega_1 - \frac{N_1 - N_2 - 1}{2}\omega_2 - \phi_1(\omega_1, \omega_2) + \phi_2(\omega_1, \omega_2) \right] \times$$

$$\exp\left\{ j\left[-\frac{M_1 + M_2}{2}\omega_1 - \frac{N_1 + N_2 + 1}{2}\omega_2 - \phi_1(\omega_1, \omega_2) - \phi_2(\omega_1, \omega_2) \right] \right\}$$

$$H_1(e^{j\omega_1}, e^{j\omega_2}) = \sin\left[-\frac{M_1 - M_2}{2}\omega_1 - \frac{N_1 - N_2 - 1}{2}\omega_2 - \phi_1(\omega_1, \omega_2) + \phi_2(\omega_1, \omega_2) \right] \times \quad (10)$$

$$\exp\left\{ j\left[-\frac{M_1 + M_2}{2}\omega_1 - \frac{N_1 + N_2 + 1}{2}\omega_2 - \phi_1(\omega_1, \omega_2) - \phi_2(\omega_1, \omega_2) + \frac{\pi}{2} \right] \right\}$$

We note from (10) that the magnitude and phase responses of $H_0(e^{j\omega_1}, e^{j\omega_2})$ and $H_1(e^{j\omega_1}, e^{j\omega_2})$ are determined by $\theta_m(\omega_1, \omega_2)$ and $\theta_p(\omega_1, \omega_2)$, where

$$\theta_m(\omega_1, \omega_2) = -\frac{M_1 - M_2}{2}\omega_1 - \frac{N_1 - N_2 - 1}{2}\omega_2 - \phi_1(\omega_1, \omega_2) + \phi_2(\omega_1, \omega_2)$$

$$\theta_p(\omega_1, \omega_2) = -\frac{M_1 + M_2}{2}\omega_1 - \frac{N_1 + N_2 + 1}{2}\omega_2 - \phi_1(\omega_1, \omega_2) - \phi_2(\omega_1, \omega_2) \quad (11)$$

Moreover, we have from (11) that

$$\phi_i(\omega_1, \omega_2) = -\frac{M_i}{2}\omega_1 - \frac{N_i + (i-1)}{2}\omega_2 - \frac{\theta_p(\omega_1, \omega_2) - (-1)^i \theta_m(\omega_1, \omega_2)}{2} \quad (12)$$

for $i = 1, 2$. (12) shows that $\phi_i(\omega_1, \omega_2)$ can be determined by $\theta_m(\omega_1, \omega_2)$ and $\theta_p(\omega_1, \omega_2)$. Hence, the desired response $\phi_{i,d}(\omega_1, \omega_2)$ can be obtained from (12) by specifying the desired $\theta_m(\omega_1, \omega_2)$ and $\theta_p(\omega_1, \omega_2)$. Since $H_1(z_1, z_2) = H_0(z_1, -z_2)$, we have $H_0(e^{j\omega_1}, e^{j(\omega_2-\pi)}) = H_1(e^{j\omega_1}, e^{j\omega_2})$. Hence, (6) becomes

$$\left| H_0(e^{j\omega_1}, e^{j\omega_2}) + H_0(e^{j\omega_1}, e^{j(\omega_2-\pi)}) \right| = 1, \text{ for } \forall (\omega_1, \omega_2),$$

$$\left| H_0(e^{j\omega_1}, e^{j\omega_2}) \right|^2 + \left| H_0(e^{j\omega_1}, e^{j(\omega_2-\pi)}) \right|^2 = 1, \text{ for } \forall (\omega_1, \omega_2), \quad (13)$$

World Academy of Science, Engineering and Technology
International Journal of Computer and Information Engineering
Vol:8, No:7, 2014

The attractive properties indicate that $H_0(e^{j\omega_1}, e^{j\omega_2})$ possesses the DC symmetry with respect to the half-band frequency $(\omega_1, \omega_2) = (0, \pi/2)$ in the upper half of the 2-D frequency plane. Moreover, (13) reveals that if $|H_0(e^{j\omega_1}, e^{j\omega_2})|$ equals zero in the stop-band, then $|H_0(e^{j\omega_1}, e^{j\omega_2})|$ equals one in the pass-band, and vice versa. Therefore, we only need to approximate the pass-band or stop-band response when designing $H_0(z_1, z_2)$. These advantages reduce the amount of numerical computation required for design and implementation.

D. Minimax Design Formulation

From (7) and (8), we note that the frequency response of the proposed 2-D PQMF bank is given by

$$T(e^{j\omega_1}, e^{j\omega_2}) = \frac{1}{2} e^{-j\omega_2} A_1(e^{j\omega_1}, e^{j\omega_2}) A_2(e^{j\omega_1}, e^{j\omega_2}) = \frac{1}{2} \exp\{j(\theta_1(\omega_1, \omega_2) + \theta_2(\omega_1, \omega_2) - \omega_2)\} \quad (14)$$

$$= \frac{1}{2} \exp\{j(-(M_1 + M_2)\omega_1 - (N_1 + N_2 + 1)\omega_2 - 2[\phi_1(\omega_1, \omega_2) + \phi_2(\omega_1, \omega_2)])\}$$

Let the desired group delays of (14) be $g_1 = M_1 + M_2$ and $g_2 = N_1 + N_2 + 1$ in the ω_1 and ω_2 axes, respectively. According to (10), and (14), the phase responses for the 2-D recursive DAFs $A_1(z_1, z_2)$ and $A_2(z_1, z_2)$ must satisfy the following constraints:

$$\begin{cases} \theta_1(\omega_1, \omega_2) + \theta_2(\omega_1, \omega_2) - \omega_2 = -g_1\omega_1 - g_2\omega_2, \text{ for } \forall (\omega_1, \omega_2) \\ \theta_1(\omega_1, \omega_2) - \theta_2(\omega_1, \omega_2) + \omega_2 = 0, \text{ for } (\omega_1, \omega_2) \in \Omega_P \\ \theta_1(\omega_1, \omega_2) - \theta_2(\omega_1, \omega_2) + \omega_2 = \pi, \text{ for } (\omega_1, \omega_2) \in \Omega_S \end{cases} \quad (15)$$

where Ω_p and Ω_s denote the pass-band and stop-band of $H_0(e^{j\omega_1}, e^{j\omega_2})$, respectively. Hence, the desired phase responses for the 2-D DAFs $A_1(z_1, z_2)$ and $A_2(z_1, z_2)$ can be set to

$$\theta_{1d}(\omega_1, \omega_2) = \begin{cases} -[(M_1 + M_2)\omega_1 + (N_1 + N_2 + 1)\omega_2]/2, & \text{for}(\omega_1, \omega_2) \in \Omega_P \\ -[(M_1 + M_2)\omega_1 + (N_1 + N_2 + 1)\omega_2 - \pi]/2, & \text{for}(\omega_1, \omega_2) \in \Omega_S \end{cases}$$

$$\theta_{2d}(\omega_1, \omega_2) = \begin{cases} -[(M_1 + M_2)\omega_1 + (N_1 + N_2 - 1)\omega_2]/2, & \text{for}(\omega_1, \omega_2) \in \Omega_P \\ -[(M_1 + M_2)\omega_1 + (N_1 + N_2 - 1)\omega_2 + \pi]/2, & \text{for}(\omega_1, \omega_2) \in \Omega_S \end{cases} \quad (16)$$

The desired phase responses for $D_1(z_1, z_2)$ and $D_2(z_1, z_2)$ can be obtained from (9) and (16) as follows:

$$\phi_{1d}(\omega_1, \omega_2) = \begin{cases} -[(M_1 - M_2)\omega_1 + (N_1 - N_2 - 1)\omega_2]/4, & \text{for}(\omega_1, \omega_2) \in \Omega_P \\ -[(M_1 - M_2)\omega_1 + (N_1 - N_2 - 1)\omega_2 + \pi]/4, & \text{for}(\omega_1, \omega_2) \in \Omega_S \end{cases}$$

$$\phi_{2d}(\omega_1, \omega_2) = \begin{cases} -[(M_2 - M_1)\omega_1 + (N_2 - N_1 + 1)\omega_2]/4, & \text{for}(\omega_1, \omega_2) \in \Omega_P \\ -[(M_2 - M_1)\omega_1 + (N_2 - N_1 + 1)\omega_2 - \pi]/4, & \text{for}(\omega_1, \omega_2) \in \Omega_S \end{cases} \quad (17)$$

respectively. From (17), we note that

$$\phi_{1d}(\omega_1, \omega_2) + \phi_{2d}(\omega_1, \omega_2) = 0, \quad \text{for} \quad \forall \ (\omega_1, \omega_2). \quad (18)$$

From (14), we observe that the proposed 2-D recursive PQMF bank $T(e^{j\omega_1}, e^{j\omega_2})$ possesses the following desired frequency characteristics if the desired condition given by (18) is satisfied

$$T(e^{j\omega_1}, e^{j\omega_2}) = \frac{1}{2} \exp\{j(-(M_1 + M_2)\omega_1 - (N_1 + N_2 + 1)\omega_2)\}. \quad (19)$$

From (13) and (18), we can see that the design problem for the proposed 2-D recursive PQMF bank is finding the real coefficients $d_i(m,n)$ of $A_i(z_1, z_2)$ such that the following two constraints can be approximately met in the minimax sense:

(i) $\phi_1(\omega_1, \omega_2) + \phi_2(\omega_1, \omega_2) = 0$, for $\forall (\omega_1, \omega_2)$,

(ii) $H_0(e^{j\omega_1}, e^{j\omega_2}) = 0$, for $(\omega_1, \omega_2) \in \Omega_s$. (20)

For a practical design, the ideal frequency band splitting for 2-D PQMF banks with sampling pattern given by **M** is shown by Fig. 4, where ω_p and ω_q are two band edge frequencies. As to the stability of $A_i(z_1, z_2)$, the stability constraints guaranteeing the stability of $A_i(z_1, z_2)$ are summarized as follows [9]: (i) $\theta_i(\omega_1, \omega_2)$ is monotonically decreasing along ω_1 axis and $\theta_i(\pi, \omega_2) = \theta_i(0, \omega_2) - M_i\pi$ for $-\pi \leqq \omega_2 \leqq \pi$; (ii) $\theta_i(\omega_1, \omega_2)$ is monotonically decreasing along ω_2 axis and $\theta_i(\omega_1, \pi) = \theta_i(\omega_1, 0) - N_i\pi$ for $-\pi \leqq \omega_1 \leqq \pi$. For simplicity, by specifying the desired phase response $\phi_{i,d}(\omega_1, \omega_2)$ to satisfy the stability constraints, we can neglect the stability problem and focus on the approximation problem given by (20) only. As a result, we can formulate the minimax design problem as follows:

$$\text{Minimize} \left| \phi_1(\omega_1, \omega_2) + \phi_2(\omega_1, \omega_2) \right|_\infty + \alpha \left| W_p(\omega_1, \omega_2) H_0(\omega_1, \omega_2) \right|_\infty, \quad (21)$$

where $|x|_\infty$ denotes the Chebyshev norm of x, α is the relative weight between the two peak error terms, and $W_p(\omega_1, \omega_2)$ is a preset weighting function with value one in Ω_S and zero in Ω_P.

III. PROPOSED DESIGN METHOD

A. Frequency Sampling and Approximation Scheme

Using the property of $\tan^{-1}(x) + \tan^{-1}(y) = \tan^{-1}\{(x+y)/(1-xy)\}$, we rewrite the first constraint of (20) for $\forall (\omega_1, \omega_2)$, as follows:

$$| \phi_1(\omega_1, \omega_2) + \phi_2(\omega_1, \omega_2) |_\infty = |\tan^{-1}(\text{Aprx1}(\mathbf{d}, \omega_1, \omega_2))|_\infty$$

$$= \left| \tan^{-1} \left\{ \frac{S_1(\omega_1, \omega_2)C_2(\omega_1, \omega_2) + C_1(\omega_1, \omega_2)S_2(\omega_1, \omega_2)}{C_1(\omega_1, \omega_2)S_2(\omega_1, \omega_2) - S_1(\omega_1, \omega_2)C_2(\omega_1, \omega_2)} \right\} \right|_\infty, \quad (22)$$

where $d_i(0,0) = 1$ for simplicity, $\mathbf{d} = [d_1(1,0), d_1(2,0), \ldots, d_2(1,0), d_2(2,0), \ldots]^T$ is the $(M_1 + (2M_1+1)\lfloor N_1/2 \rfloor + M_2 + (2M_2+1)\lfloor N_2/2 \rfloor) \times 1$ coefficient vector, where the superscript T denotes the transpose operation. And

$$S_i(\omega_1, \omega_2) = \sum \sum_{(m,n) \in \Re_i} d_i(m,n) \sin(m\omega_1 + n\omega_2)$$

$$C_i(\omega_1, \omega_2) = \sum \sum_{(m,n) \in \Re_i} d_i(m,n) \cos(m\omega_1 + n\omega_2) \quad , i = 1, 2.$$

(23)

World Academy of Science, Engineering and Technology
International Journal of Computer and Information Engineering
Vol:8, No:7, 2014

Minimizing (22) is equivalent to minimizing the following term

$$\left\| \left\{ \frac{S_1(\omega_1,\omega_2)C_2(\omega_1,\omega_2)+C_1(\omega_1,\omega_2)S_2(\omega_1,\omega_2)}{C_1(\omega_1,\omega_2)S_2(\omega_1,\omega_2)-S_1(\omega_1,\omega_2)C_2(\omega_1,\omega_2)} \right\} \right\|_{\infty} \quad (24)$$

since the inverse tangent function is a monotonic function. The second constraint of (20) can be rewritten as

$$|H_0(e^{j\omega_1},e^{j\omega_2})|_{\infty}=|\text{Aprx2}(\mathbf{d},\omega_1,\omega_2)|_{\infty}=$$

$$\left| \frac{e^{-jM_1\omega_1}e^{-jN_1\omega_2}\left(\sum\sum_{(m,n)\in\Re_1}d_1(m,n)e^{j(m\omega_1+n\omega_2)}\right)}{\left(\sum\sum_{(m,n)\in\Re_1}d_1(m,n)e^{-j(m\omega_1+n\omega_2)}\right)}+\frac{e^{-jM_2\omega_1}e^{-j(N_2+1)\omega_2}\left(\sum\sum_{(m,n)\in\Re_2}d_2(m,n)e^{j(m\omega_1+n\omega_2)}\right)}{\left(\sum\sum_{(m,n)\in\Re_2}d_2(m,n)e^{-j(m\omega_1+n\omega_2)}\right)} \right|_{\infty} \quad (25)$$

Utilizing the LLCY algorithm of [10], we reformulate the minimization problem of (21) as follows:

$$\textit{Minimize} \left\{ \begin{array}{l} W_{ls1}(\omega_1,\omega_2)|\text{Aprx1}(\mathbf{d},\omega_1,\omega_2)|^2 \\ +\alpha W_p(\omega_1,\omega_2)W_{ls2}(\omega_1,\omega_2)|\text{Aprx2}(\mathbf{d},\omega_1,\omega_2)|^2 \end{array} \right\}, \quad (26)$$

where $W_{ls1}(\omega_1,\omega_2)$ and $W_{ls2}(\omega_1,\omega_2)$ are two required least-squares weighting functions. Let the frequency pair $(\omega_{1r},\omega_{2r})$ represent the rth uniformly sampled frequency grid point in the interested frequency band. And $1 \leqq r \leqq R$, where R represents the total number of uniformly sampled frequency grid points. The design process of the proposed method is then performed on the R frequency grid points. If the number R of grid points is sufficiently large, the obtained best approximation solution of the objective function based on the grid points will be close to the best solution found based on (26). This conclusion can be justified by the theorem due to Cheney [11, Chapter 3]. We utilize a linearization scheme to approximate the related errors of (22) and (25) due to a perturbation in the filter coefficient vector $\mathbf{d}$ in the linear subspace spanned by the gradient matrix associated with $\text{Aprx1}(\mathbf{d},\omega_{1r},\omega_{2r})$ and $\text{Aprx2}(\mathbf{d},\omega_{1r},\omega_{2r})$. As a result, the approximation for minimizing (21) can be formulated as finding the increments $\delta\mathbf{d}_k=[\delta d_{1k}(1,0),$ $\delta d_{1k}(2,0), \ldots, \delta d_{2k}(1,0), \delta d_{2k}(2,0)\ldots]^T$ of the filter coefficient vectors $\mathbf{d}$ at the kth iteration such that

$$|\text{Aprx1}(\mathbf{d}_k,\omega_{1r},\omega_{2r})+\delta\mathbf{d}_k^T\triangledown\text{Aprx1}(\mathbf{d}_k,\omega_{1r},\omega_{2r})|_{\infty}+\alpha W_p(\omega_{1r},\omega_{2r})|$$
$$\text{Aprx2}(\mathbf{d}_k,\omega_{1r},\omega_{2r})+\delta\mathbf{d}_k^T\triangledown\text{Aprx2}(\mathbf{d}_k,\omega_{1r},\omega_{2r})|_{\infty} \quad (27)$$

is minimized for all $(\omega_{1r},\omega_{2r})$, where the subscript k denotes the results obtained at the kth iteration, $\triangledown\text{Aprx1}(\mathbf{d}_k,\omega_{1r},\omega_{2r})$ and $\triangledown\text{Aprx2}(\mathbf{d}_k,\omega_{1r},\omega_{2r})$ are the gradient vectors of $\text{Aprx1}(\mathbf{d}_k,\omega_{1r},\omega_{2r})$ and $\text{Aprx2}(\mathbf{d}_k,\omega_{1r},\omega_{2r})$ with respect to the filter coefficient vector $\mathbf{d}_k$, respectively, and are given by

$$\triangledown\text{Aprx1}(\mathbf{d}_k,\omega_{1r},\omega_{2r})=[\psi_1(\omega_{1r},\omega_{2r},1)\ \psi_1(\omega_{1r},\omega_{2r},2)\ \ldots\ ]^T,$$

$$\triangledown\text{Aprx2}(\mathbf{d}_k,\omega_{1r},\omega_{2r})=[\psi_2(\omega_{1r},\omega_{2r},1)\ \psi_2(\omega_{1r},\omega_{2r},2)\ \ldots\ ]^T, \quad (28)$$

where $\psi_1(\omega_{1r},\omega_{2r},j)=\partial\text{Aprx1}(\mathbf{d}_k,\omega_{1r},\omega_{2r})/\partial d_k(j)$ is the jth gradient component of $\text{Aprx1}(\mathbf{d}_k,\omega_{1r},\omega_{2r})$, $\psi_2(\omega_{1r},\omega_{2r},j)=\partial\text{Aprx2}(\mathbf{d}_k,\omega_{1r},\omega_{2r})/\partial d_k(j)$ is the jth gradient component of $\text{Aprx2}(\mathbf{d}_k,\omega_{1r},\omega_{2r})$, and $d_k(j)$ is the jth entry of the coefficient vector $\mathbf{d}_k$ obtained at the kth iteration. Accordingly, we have an approximate minimization problem for (26) as follows:

$$\textit{Minimize } J=(\mathbf{U}_1\delta\mathbf{d}_k-\mathbf{s}_1)^T\mathbf{W}_{ls1}(\mathbf{U}_1\delta\mathbf{d}_k-\mathbf{s}_1)+\alpha(\mathbf{U}_2\delta\mathbf{d}_k-\mathbf{s}_2)^T$$
$$\mathbf{W}_p\mathbf{W}_{ls2}(\mathbf{U}_2\delta\mathbf{d}_k-\mathbf{s}_2), \quad (29)$$

where $\mathbf{U}_i$ is a $R\times(M_1+(2M_1+1)\lfloor N_1/2\rfloor+M_2+(2M_2+1)\lfloor N_2/2\rfloor)$ matrix with the (l,n)th entry given by $U_i(l,n)=\psi_i(\omega_{1l},\omega_{2l},n)$, $1\leq l\leq R$, $1\leq n\leq(M_1+(2M_1+1)\lfloor N_1/2\rfloor+M_2+(2M_2+1)\lfloor N_2/2\rfloor)$, $\mathbf{s}_i$ is a $R\times1$ column vector with the lth entry given by $s_i(l)=-\text{Aprx}i(\mathbf{d}_k,\omega_{1l},\omega_{2l})$, $1\leq l\leq R$, $\mathbf{W}_{lsi}=diag\{W_{lsi}(\omega_{11},\omega_{21}),$ $W_{lsi}(\omega_{12},\omega_{22}),\ldots,W_{lsi}(\omega_{1R},\omega_{2R})\}$ denotes the $R\times R$ diagonal matrix containing the required least-squares weighting function calculated at $(\omega_{1r},\omega_{2r})$, $r=1,2,\ldots,R$, of the R frequency grid points, for $i=1,2$, and $\mathbf{W}_p$ represents the $R\times R$ diagonal matrix containing the preset weighting function with value one at $(\omega_{1r},\omega_{2r})$ in Ω_S and zero at $(\omega_{1r},\omega_{2r})$ in Ω_P. The optimal solution for minimizing the objective function J of (29) is given by

$$\delta\mathbf{d}_k=[\text{Re}\{(\mathbf{U}_1^T\mathbf{W}_{ls1}\mathbf{U}_1+\alpha\mathbf{U}_2^T\mathbf{W}_p\mathbf{W}_{ls2}\mathbf{U}_2)\}]^{-1}\times\text{Re}\{(\mathbf{U}_1^T\mathbf{W}_{ls1}\mathbf{s}_1+\alpha$$
$$\mathbf{U}_2^T\mathbf{W}_p\mathbf{W}_{ls2}\mathbf{s}_2)\}, \quad (30)$$

where $\text{Re}\{x\}$ denotes the real part of x. The suitable least-squares weighting function $W_{lsi}(\omega_{1r},\omega_{2r})$, $r=1,2,\ldots,R$, $i=1,2$, required in (30) for producing a quasi-equiripple design can be obtained by utilizing the LLCY algorithm of [10].

B. Iterative Design Procedure

Step 1: Initiation:
<1.1> Determine the design parameters: the orders M_i and N_i, $i=1,2$, the relative weight α, band edge frequencies ω_p and ω_q.
<1.2> Set the zero vector as an initial guess for the vector $\mathbf{d}$.
<1.3> Set the iteration number $k=0$.
Step 2: Perform a test for stopping the iteration process:
<2.1> Compute $V_k=|\text{Aprx1}(\mathbf{d}_k,\omega_1,\omega_2)|_{\infty}+\alpha|\text{Aprx2}(\mathbf{d}_k,\omega_1,\omega_2)|_{\infty}$.
<2.2> Terminate the design process and take the coefficient vector $\mathbf{d}_k$ as the designed filter coefficient vector if $|V_k-V_{k+1}|/|V_k|\leqq\varepsilon$, where ε is a preset small positive real number. Otherwise, go to *Step 3* to perform an inner iterative process for finding the best increment $\delta\mathbf{d}_k$ of the filter coefficient vector $\mathbf{d}_k$.
Step 3: Calculate the increment $\delta\mathbf{d}_k$ of $\mathbf{d}_k$ at the kth iteration from (30) according to the LLCY iterative algorithm as follows:
<3.1> Set the initial weighting matrix $\mathbf{W}_{lsi}$ to the $R\times R$ identity matrix $\mathbf{I}$ and an inner iteration index $p=0$.
<3.2> Compute the WLS solution $\delta\mathbf{d}_k$ from (30). Set $\delta\mathbf{d}_k^{(p)}=\delta\mathbf{d}_k$, where the superscript p denotes the $\delta\mathbf{d}_k$ obtained at the pth iteration during the inner iteration process.

World Academy of Science, Engineering and Technology
International Journal of Computer and Information Engineering
Vol:8, No:7, 2014

<3.3> Compute the error functions $e_{1k}^{(p)}(\omega_1,\omega_2) = (\mathbf{U}_1\delta\mathbf{d}_k^{(p)} - \mathbf{s}_1)$ and $e_{2k}^{(p)}(\omega_1,\omega_2) = (\mathbf{U}_2\delta\mathbf{d}_k^{(p)} - \mathbf{s}_2)$.

<3.4> Let $G_i^{(p)}(J) = |e_{ik}^{(p)}(\omega_{1J},\omega_{2J})|$, where $G_i^{(p)}(J) > |e_{ik}^{(p)}(\omega_{1(J+1)},\omega_{2(J+1)})|$ and $G_i^{(p)}(J) > |e_{ik}^{(p)}(\omega_{1(J-1)},\omega_{2(J-1)})|$. If $|\max\{G_i^{(p)}(J)\} - \max\{G_i^{(p-1)}(J)\}|/\max\{G_i^{(p-1)}(J)\} \leqq \eta_i$, where each η_i is a preset small real number, the WLS solution $\delta\mathbf{d}_k$ is used for obtaining the optimal solution of $\mathbf{d}$, This ends the inner iterative process. Then, go to *Step 4*. Otherwise, go to <3.5>.

<3.5> Update the least-squares weighting function $W_{lsi}(\omega)$ according to the systematical approach as described in [10] and set the iteration index $p = p + 1$. Then, go to <3.2>.

Step 4: Update the filter coefficient vector as follows:

<4.1> Use the obtained optimal solution $\delta\mathbf{d}_k$ to find the best increment such that the following term is minimized.

$|\text{Aprx1}(\mathbf{d}_k+\beta\delta\mathbf{d}_k,\omega_1,\omega_2)|_\infty + \alpha|\text{Aprx2}(\mathbf{d}_k+\beta\delta\mathbf{d}_k,\omega_1,\omega_2)|_\infty$, all $\beta \geqq 0$.

<4.2> Utilize the simplex algorithm of [12] to perform the line search for finding the best value of β. Let the best β be β_k.

<4.3> Update the filter coefficient vector according to

$$\mathbf{d}_{(k+1)} = \mathbf{d}_k + \beta_k\delta\mathbf{d}_k.$$

<4.4> Set $k = k + 1$ and go to *Step 2*.

IV. SIMULATION RESULTS

We present simulation results for illustration and comparison. The performance of the designed 2-D recursive PQMF bank is evaluated in terms of the minimum stop-band attenuation (MSA) of $H_0(z_1,z_2)$, the pass-band magnitude mean-squared error (PMSE) of $H_0(z_1,z_2)$, the stop-band magnitude mean-squared error (SMSE) of $H_0(z_1,z_2)$, the maximum variation in phase response (MVPR$_i$) of $D_i(e^{j\omega_1},e^{j\omega_2})$ in the pass-band, and the peak phase error (PPE) of the designed PQMF bank $T(e^{j\omega_1},e^{j\omega_2})$. They are defined as follows:

$$\text{MSA} = -\max_{(\omega_1,\omega_2)\in\Omega_s}\left(20\log_{10}\left(\left\|H_0\left(e^{j\omega_1},e^{j\omega_2}\right)\right\|\right)\right) \quad \text{(dB)}$$

$$\text{PMSE} = \frac{\sum\sum_{(\omega_1,\omega_2)\in\Omega_p}\left(\left|H_0(e^{j\omega_1},e^{j\omega_2})\right| - \left|H_{0,d}(\omega_1,\omega_2)\right|\right)^2}{\text{number of grid points in the pass-band}}$$

$$\text{SMSE} = \frac{\sum\sum_{(\omega_1,\omega_2)\in\Omega_s}\left(\left|H_0(e^{j\omega_1},e^{j\omega_2})\right| - \left|H_{0,d}(\omega_1,\omega_2)\right|\right)^2}{\text{number of grid points in the stop-band}}$$

$$\text{MVPR}_i = \max_{(\omega_1,\omega_2)\in\Omega_P}\left|\arg\{D_i(e^{j\omega_1},e^{j\omega_2})\} - \phi_{id}(\omega_1,\omega_2)\right| \quad \text{(radian)}$$

$$\text{PPE} = \max_{(\omega_1,\omega_2)}\left|\arg\{T(e^{j\omega_1},e^{j\omega_2})\} + g_1\omega_1 + g_2\omega_2\right| \quad \text{(radian)}$$

Example: Using the same magnitude characteristic as that of [5], we set the band edge frequencies $\omega_p = \omega_q = 0.8\pi$. Accordingly, the desired magnitude response of $H_0(z_1,z_2)$ possesses the symmetry with respect to the frequency $(0, 0.5\pi)$. Therefore, about half of the coefficients can be set to zero and only uniformly sampled pass-band frequency grid points are considered during the design procedure. The 2-D DC filters $H_0(z_1,z_2)$ and $H_1(z_1,z_2)$ are obtained by setting $M_1 = M_2 = 6$ and $N_1 = N_2 = 8$. Then, the ideal group delays are $g_1 = M_1 + M_2 = 12$

and $g_2 = N_1 + N_2 + 1 = 17$. We design the 2-D NSHP DAF $A_i(z_1,z_2)$ whose denominator phase $\arg\{D_i(e^{j\omega_1},e^{j\omega_2})\}$ with the desired passband phase response $\phi_{i,d}(\omega_1,\omega_2)$ obtained by substituting $\theta_{m,d}(\omega_1,\omega_2) = 0$ and $\theta_{p,d}(\omega_1,\omega_2) = -(M_1+M_2)\omega_1/2 - (N_1+N_2+1)\omega_2/2$ into (12). The resulting $\phi_{i,d}(\omega_1,\omega_2)$ are given by

$$\phi_{1d}(\omega_1,\omega_2) = \begin{cases} \omega_2/4, & \text{for}(\omega_1,\omega_2)\in\Omega_P \\ \omega_2/4 - \pi/4, & \text{for}(\omega_1,\omega_2)\in\Omega_S \end{cases}$$

$$\phi_{2d}(\omega_1,\omega_2) = \begin{cases} -\omega_2/4, & \text{for}(\omega_1,\omega_2)\in\Omega_P \\ -\omega_2/4 + \pi/4, & \text{for}(\omega_1,\omega_2)\in\Omega_S \end{cases} \quad (31)$$

Since $\phi_{i,d}(\omega_1,\omega_2)$ of (31) are two functions of ω_2 only and satisfy the stability conditions, we can omit the stability issue and focus the design problem shown by (21). Moreover, the designed analysis/synthesis filters can achieve approximately linear-phase responses in the pass-band because of the ideal phase specification given by $\theta_{p,d}(\omega_1,\omega_2) = -(M_1+M_2)\omega_1/2 - (N_1+N_2+1)\omega_2/2$. The parameters used for this design are chosen by experiment and given as follows: $\eta_1 = \eta_2 = 1.0\times10^{-4}$, $\alpha = 5$, and $\varepsilon = 1\times10^{-3}$. The spacing between two adjacent frequency grid points is the same as that used by [5] and set to $2\pi/64$. Significant design results are shown in Table I for comparison. The magnitude responses of the analysis filters are depicted in Fig. 5 and the resulting phase error of $A_i(z_1,z_2)$ is depicted in Fig. 6. The resulting phase error of the designed 2-D recursive PQMF bank is shown in Fig. 7. From Table I, we observe that the proposed method can design the filter coefficients for the 2-D NSHP DAFs $A_i(z_1,z_2)$, for $i = 1, 2$ simultaneously and provide a 2-D recursive PQMF bank with frequency responses better than those of [5].

V. CONCLUSION

This paper has presented a novel technique for the minimax design of two-channel recursive parallelogram quadrature mirror filter (PQMF) banks. The proposed analysis/synthesis filters possess a 2-D doubly complementary (DC) property. The PQMF bank can achieve the nearly linear-phase response without magnitude distortion, the aliasing artifacts, and an extra phase equalizer. Using the weighted least-squares (WLS) algorithm, the proposed PQMF bank can be efficiently designed. The design results show that the proposed method provides more satisfactory design than the existing techniques.

TABLE I
THE SIGNIFICANT DESIGN RESULTS

	Proposed Method	Method of [5]
MSA(dB)	28.1350	23.2292
PMSE	9.3093×10^{-8}	7.3647×10^{-7}
SMSE	4.5983×10^{-4}	1.2800×10^{-3}
MVPR1	3.9142×10^{-2}	5.9370×10^{-2}
MVPR2	2.3284×10^{-2}	1.8531×10^{-2}
PPE	0.0826	0.1386
Number of Independent Coefficients	58,58	45,45,22

World Academy of Science, Engineering and Technology
International Journal of Computer and Information Engineering
Vol:8, No:7, 2014

(a) Analysis Bank   (b) Synthesis Bank
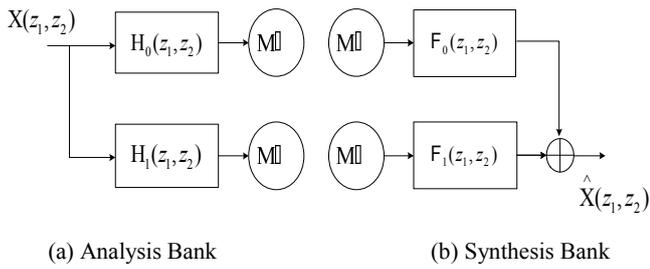
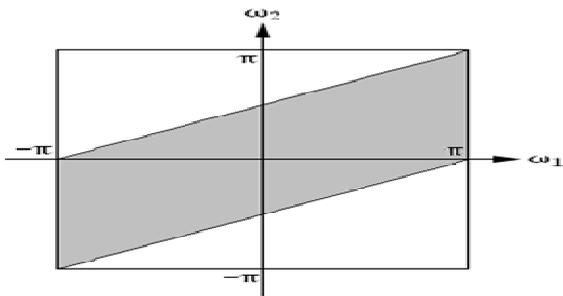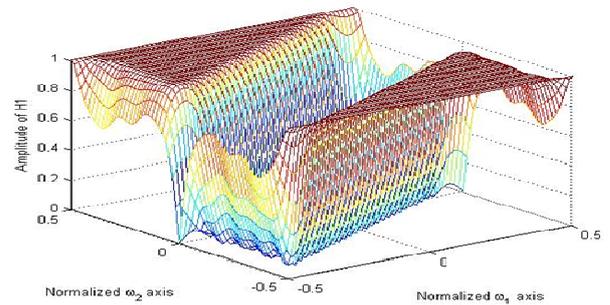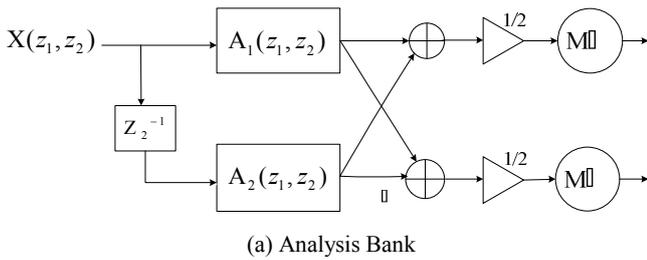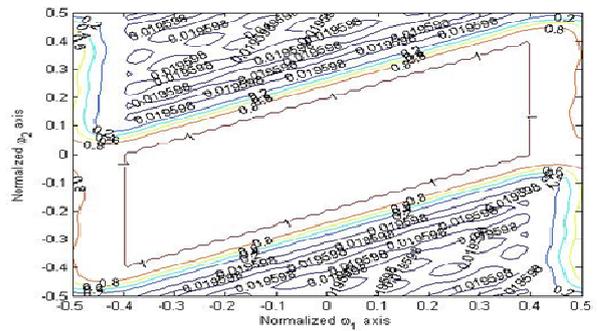Fig. 1 The conventional two-channel PQMF bank

Fig. 2 The Ideal Frequency Band-Splitting for 2-D PQMF bank
Pass-band region: Shadow area. Stop-band region: White area

(a) Analysis Bank
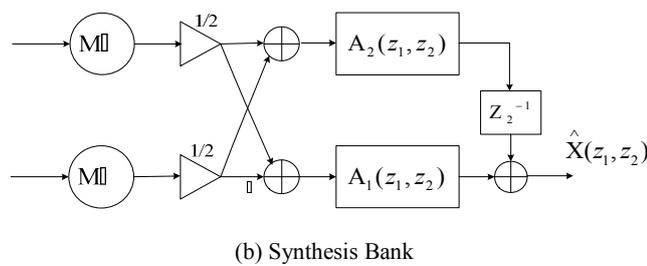

(b) Synthesis Bank

Fig. 3 The proposed Analysis/Synthesis banks

Fig. 4 The ideal frequency band splitting. Ω_p: gray shadow area. Ω_s: dark shadow area. The white area represents the transition region

(a) Perspective plot of $\left|H_0(e^{j\omega_1}, e^{j\omega_2})\right|$

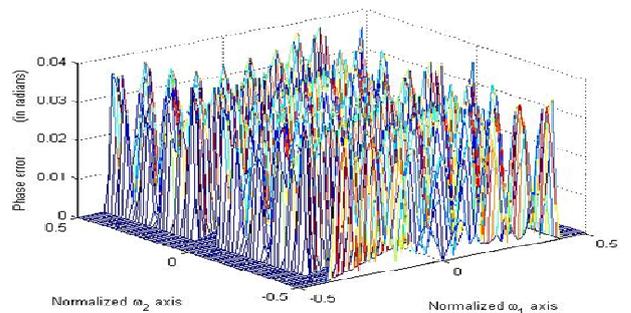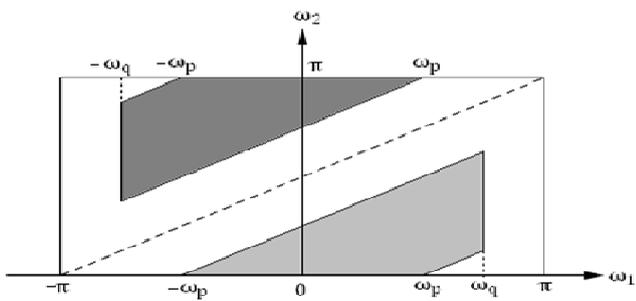(b)   Perspective plot of $\left|H_1(e^{j\omega_1}, e^{j\omega_2})\right|$

(c) Contour plot of $\left|H_0(e^{j\omega_1}, e^{j\omega_2})\right|$ (the solid lines: the band edges).

Fig. 5 Magnitude responses of analysis filters

(a) $i = 1$

World Academy of Science, Engineering and Technology
International Journal of Computer and Information Engineering
Vol:8, No:7, 2014

[12] J. A. Nelder and R. A. Meade, "Simplex method for function minimization," *Comput. J.*, no. 7, pp. 308-313, 1965.
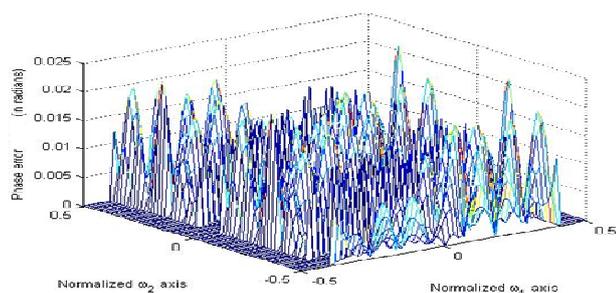
(b) $i = 2$

Fig. 6 Phase errors $\left| \arg\{D_i(e^{j\omega_1}, e^{j\omega_2})\} - \phi_{id}(\omega_1, \omega_2) \right|$ for $i = 1, 2$
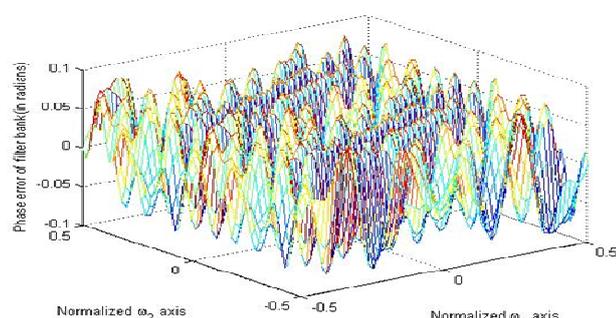

Fig. 7 Phase error $\left| \arg\{T(e^{j\omega_1}, e^{j\omega_2})\} + g_1\omega_1 + g_2\omega_2 \right|$

REFERENCES

[1] S. I. Park, M. J. Smith, and R. M. Mersereau, "Improved structure of maximally decimated directional filter banks for spatial image analysis," *IEEE Trans. on Image Processing*, vol. 13, pp. 1424–1431, Nov. 2004.
[2] T. T. Nguyen and S. Oraintara, "Multiresolution direction filter banks: Theory, design and application," *IEEE Trans. on Signal Processing*, vol. 53, pp. 3895–3905, Oct. 2005.
[3] Z. Lei and A. Makur, "Two-dimensional antisymmetric linear phase filter bank construction using symmetric completion," *IEEE Trans. on Circuits and Systems-II: Express Briefs*, vol. 54, no. 1, pp. 57-60, Jan. 2007.
[4] P. G. Patwardhan, B. Patil, and V. M. Gadre, "Polyphase conditions and structures for 2-D quincunx FIR filter banks having quadrantal or diagonal symmetries," *IEEE Trans. on Circuits and Systems-II: Express Briefs* vol. 54, no. 9, pp. 790-794, Sept. 2007.
[5] J.-H. Lee, and Y.-H. Yang, "Two-channel parallelogram QMF banks using 2-D NSHP digital allpass filters," *IEEE Trans. on Circuits and Systems I: Regular Papers*, vol. 57, no. 9, pp. 2498-2508, Sept. 2010.
[6] M. Vetterli and G. Karlsson, "Theory of two-dimensional multirate filter banks," *IEEE Trans. on Acoustics, Speech and Signal Processing*, vol. 38, no. 6, pp. 925-937, Nov. 1990.
[7] P. Siohan, "2-D FIR filter design for sampling structure conversion," *IEEE Trans. on Circuits and Systems for Video Technology*, vol. 1, no. 4, pp. 337-350, Dec. 1991.
[8] A. Knoll, "Filter design for the interpolation of highly subsampled pictures," *Signal Processing: Image Communication*, vol. 3, no. 2-3, pp. 239-248, June 1991.
[9] S. C. Pei and J. J. Shyu, "Eigenfilter design of 1-D and 2-D IIR digital all-pass filters," *IEEE Trans. on Signal Processing*, vol. 42, no. 4, pp. 966-968, Apr. 1994.
[10] Y.C. Lim, J.-H. Lee, C.-K. Chen, and R.H. Yang, "A weighted least squares algorithm for quasi-equiripple FIR and IIR digital filter design," *IEEE Trans. on Signal Processing*, vol. 40, pp. 551-558, Mar. 1992.
[11] E. W. Cheney, *Introduction to Approximation Theory*, New York: Mc-Graw-Hill, 1966.